Dynamic Analysis and Control of UPFC using Transient Simulation

R. Caldon, P. Mattavelli
Department of Electrical Engineering
University of Padova
Via Gradenigo 6/a, 35131 Padova – ITALY
caldon@light.dei.unipd.it - pmatta@tania.dei.unipd.it

B.M. Han
Department of Electrical and Electronic Engineering
Myongij University
Seoul-KOREA
erichan@wh.myongji.ac.kr

Abstract. **A control structure for the Unified Power Flow Controller (UPFC) based on multipulse Neutral Point Clamped (NPC) Inverters is proposed and the relevant dynamic analysis is described. In particular, attention is focused on the control design for both shunt and series converters, together with a new solution for the regulator of the dc link voltage sharing across dc capacitors of the multilevel inverters. For such purpose, an energy-based approach, which uses the notion of incremental energy and passivity, is investigated. In order to test this approach, a detailed UPFC model has been developed in ATP using 24-pulse NPC inverters. Simulation results about UPFC dynamic performance, effects of increasing transmission capacity and damping low-frequency oscillations are reported.**

Keywords: FACTS, UPFC, Dynamic Modeling, Multilevel Inverters, Transient Simulation.

I. INTRODUCTION

Flexible AC transmission system (FACTS) devices are finding increasing application in power systems, since they are able to control power flow, to increase transient stability, to damp power oscillations and, possibly, subsynchronous resonances. Among many FACTS devices [1] based on voltage-source inverters, the UPFC (Unified Power Flow Controller) is known as an ultimate device because it can control independently the real and reactive power flowing through transmission lines.

The steady-state performance and characteristic of UPFCs have been analysed and reported in detail in the literature [1,2,3,4,5] and are not discussed in this paper. Moreover, we will neglect typical *external* controls which set the transmission reactive and active power reference and the shunt reactive power reference based on power flow control and on voltage regulation, respectively. Instead, our attention is focused on the ac current regulation of the series and parallel currents and of the dc-link voltages of the multilevel inverters, together with a solution for damping typical low-frequency oscillations.

For the *internal* control of the UPFC we explore an energy-based approach based on notion of incremental energy [6]. This approach is aimed to achieve the ac current and dc voltage regulations shaping the energy of the closed-loop system, similarly to Lyapunov-based techniques. We propose this technique for control of parallel currents, series currents and dc link voltages (and, thus, their equalization, which is needed in order to share voltage stresses of the GTOs equally) for UPFCs based on multipulse NPC inverters, although the approach can be easily extended to other UPFC topologies.

In order to test our control approach and analyze the dynamic performance of UPFC, we have developed a detailed ATP model using 24-pulse NPC inverters. Different levels of detail are considered, such as the approximation of the ideal gate-turn off switches with switching functions and with time-averaged functions. Finally, this model has also been used to verify the UPFC damping of low-frequency oscillations in a simplified system representing a typical single machine connected to an infinite bus.

II. BASIC OPERATION AND ANALYSIS

The UPFC consists of two voltage-source inverters, which operate from common dc link capacitors and are connected with the ac transmission system through coupling transformers. The configuration, which is adopted in this paper, is shown in Fig.1 and corresponds to the actual UPFC installation in the Inez Substation [8]. Both series and shunt converters are based on three-level NPC inverters switching at fundamental frequency. The high-quality voltage waveform is obtained through multipulse (either 24 or 48-pulse) operations involving (either 4 or 8, respectively) three-phase voltage-source inverters connected together through zig-zag arrangement transformers, which allow elimination or reduction of the low order harmonics produced by inverter switching at fundamental frequency.

The circuit equations for the parallel part can be derived from the equivalent circuit of Fig. 2, where inductances L_p account for the leakage of coupling

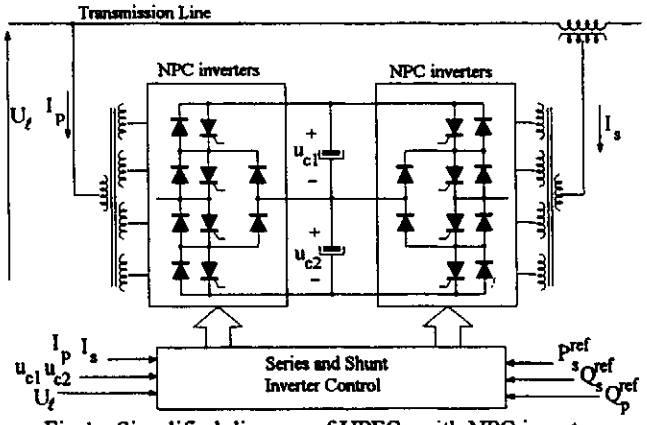

Fig.1 - Simplified diagram of UPFCs with NPC inverters

transformers, series resistance R_p for conduction losses of transformers and inverters and resistance R_c for capacitor and inverter losses.

Applying the synchronous rotating reference frame (d-q) transformation to the three-phase circuit equations of Fig.2, we can write that:

$$L_p \frac{d}{dt}\begin{bmatrix} i_{pd} \\ i_{pq} \end{bmatrix} = \begin{bmatrix} -R_p & -\omega_\ell L_p \\ \omega_\ell L_p & -R_p \end{bmatrix} \begin{bmatrix} i_{pd} \\ i_{pq} \end{bmatrix} + \begin{bmatrix} -e_{pd}+e_{\ell d} \\ -e_{pq}+e_{\ell q} \end{bmatrix} \quad (1)$$

where ω_ℓ is the line angular frequency, $i_{pk}\,(k=d,q)$ the d-q shunt currents, $e_{pk}\,(k=d,q)$ the d-q inverter voltages and $e_{\ell k}\,(k=d,q)$ the d-q line voltages; in the d-q transformation, we select the line voltage vector on the d-axis so that $e_{\ell q}$ is null. With this choice, the active power (P_p) and reactive power (Q_p) absorbed by the shunt part of the UPFC are $P_p = e_{\ell d} i_{pd}$ and $Q_p = e_{\ell d} i_{pq}$; thus, the control of the current along the d-axis corresponds to the control of the active power P_p, while the control of the q-axis current corresponds to the control of the reactive power Q_p.

Dynamic equations of the UPFC series converter strongly depend on the line configuration and they can be, in general, quite complex. In order to simplify our analysis, we assume that the transmission line can be modeled by lumped inductance L_ℓ, resistance R_ℓ and, possibly, capacitance C_ℓ, which represents the fixed series compensation, if present. With this assumption, d-q equations for the series part can be written as

$$\begin{aligned} L_{\ell T} \frac{d}{dt}\begin{bmatrix} i_{sd} \\ i_{sq} \end{bmatrix} &= \begin{bmatrix} -R_{\ell T} & -\omega_\ell L_{\ell T} \\ \omega_\ell L_{\ell T} & -R_{\ell T} \end{bmatrix} \begin{bmatrix} i_{sd} \\ i_{sq} \end{bmatrix} + \begin{bmatrix} -e_{sd}-u_{\ell d}+e_{12d} \\ -e_{sq}-u_{\ell q}+e_{12q} \end{bmatrix} \\ C_\ell \frac{d}{dt}\begin{bmatrix} u_{\ell d} \\ u_{\ell q} \end{bmatrix} &= \begin{bmatrix} 0 & -\omega_\ell C_\ell \\ \omega_\ell C_\ell & 0 \end{bmatrix} \begin{bmatrix} u_{\ell d} \\ u_{\ell q} \end{bmatrix} + \begin{bmatrix} i_{sd} \\ i_{sq} \end{bmatrix} \end{aligned} \quad (2)$$

where $L_{\ell T} = L_\ell + L_s$, $R_{\ell T} = R_\ell + R_s$ (being L_s and R_s the leakage inductance and resistance of the series transformer), $i_{sk}\,(k=d,q)$ the d-q series currents, $e_{sk}\,(k=d,q)$ the d-q series inverter voltages, $u_{\ell k}\,(k=d,q)$ the d-q capacitors voltages and $e_{12k}\,(k=d,q)$ the d-q voltage differences between the two terminals of the transmission line. Of course, if the series compensation is not present, we may just neglect the dynamic equations related to capacitance C_ℓ.

Circuit equations in the dc circuit are derived from the power balance relationship between the ac and dc side and from the mid-point currents i_{os} and i_{op}, determined by the NPC inverter switching. Taking into account that we are using the power invariant d-q transformation, from Fig. 2 it can be verified that:

$$\begin{aligned} C\frac{d}{dt}\begin{bmatrix} u_{c1} \\ u_{c2} \end{bmatrix} &= \begin{bmatrix} -1/R_c & -i_{oT}/u_{cT} \\ i_{oT}/u_{cT} & -1/R_c \end{bmatrix} \begin{bmatrix} u_{c1} \\ u_{c2} \end{bmatrix} + \\ &+ \frac{1}{u_{cT}} \sum_{k=p,s} \begin{bmatrix} e_{kd}i_{kd}+e_{kq}i_{kq} \\ e_{kd}i_{kd}+e_{kq}i_{kq} \end{bmatrix} \end{aligned} \quad (3)$$

where $u_{cT} = u_{c1} + u_{c2}$ is the total dc-link voltage and $i_{oT} = i_{os} + i_{op}$ is the total midpoint current.

Thanks to the use of multilevel inverters, even if switching at fundamental frequency, it is possible to regulate independently the d-q voltages of both the series and shunt converters. For example, for the shunt inverter we can write [9]:

$$\begin{aligned} e_{pd} &= m_p u_{cT} \cos(\alpha_p) \\ e_{pq} &= m_p u_{cT} \sin(\alpha_p) \end{aligned} \quad (4)$$

where α_p is the angle by which the inverter voltage vector leads the line voltage vector and m_p corresponds to the amplitude regulation. In fact, fundamental value of the instantaneous output voltage of a 3-level inverter, shown in Fig.3b, can be regulated, even if switched at fundamental frequency, by adjusting the zero-voltage interval γ; a simple Fourier analysis on Fig. 3b shows that the peak value of fundamental component of the phase voltage is:

$$\hat{E}_1(\gamma) = \frac{2}{\pi} u_{cT} \cos(\gamma) \quad (5)$$

which needs to be multipled [4] by $\cos(\pi/N_{pulse})$ in order to account for the multipulse transformers, being N_{pulse} the number of pulses (i.e. 24,48).

Assuming sinusoidal phase current, as shown in Fig. 3c, and balanced operation, the average mid-point current I_o is null, ensuring that the dc capacitor voltages do not unbalance during ideal steady-state conditions. However, there is a variety of different effects [7] such as unequal capacitance leakage currents, inverter dead-times, asymmetrical operation during transients and disturbances, which may contribute to the divergence of the two capacitor voltages, requiring a proper action in order to compensate such effects.

Equalization of dc voltages can be performed by unbalacing the GTO firing angles, as shown in Fig. 3d-e. Let us consider the following expression for the zero-voltage angles γ_k ($k=1..4$):

$$\begin{aligned} \gamma_1 &= \gamma + \Delta\gamma_R + \Delta\gamma_A \\ \gamma_2 &= \gamma - \Delta\gamma_R + \Delta\gamma_A \\ \gamma_3 &= \gamma - \Delta\gamma_R - \Delta\gamma_A \\ \gamma_4 &= \gamma + \Delta\gamma_R - \Delta\gamma_A \end{aligned} \quad (6)$$

where $\Delta\gamma_R$ and $\Delta\gamma_A$ are two (small) deviations of angles γ_k respect to the balanced operation. It can be easily verified that, under the assumption of small capacitor unbalance (i.e. $u_{c1} \cong u_{c2}$) and of small deviations for $\Delta\gamma_R$ and $\Delta\gamma_A$, (5) still holds. Therefore, under these

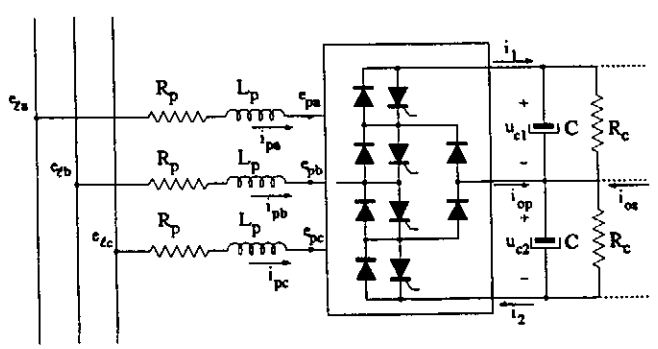

assumptions, the control of the fundamental output voltage is decoupled from the control of the mid-point voltage obtained regulating the deviation angles $\Delta\gamma_R$ and $\Delta\gamma_A$. Decomposing phase current $i(t)$ into active ($i_A(t)$) and reactive components ($i_R(t)$) as follows

$$i(t) = i_A(t) + i_R(t) = I_A \sin(\theta) - I_R \cos(\theta), \qquad (7)$$

it is easy to see that deviation $\Delta\gamma_R$ can control the midpoint current through the reactive current $i_R(t)$ (Fig. 3d) and $\Delta\gamma_A$ the midpoint current through the active current $i_A(t)$ (Fig. 3e). Adding the two contributions, the average mid-point current I_o can be written as

$$I_o = \frac{6}{\pi}\{I_A \sin(\gamma)\,\Delta\gamma_A - I_R \cos(\gamma)\,\Delta\gamma_R\} \qquad (8)$$

It is worth noting that this approach allows the control of the average value of the mid-point current I_o, decoupled from the control of the fundamental voltage, even if the reactive power absorbed by the UPFC is null. This is an improvement in comparison with the solution reported in [7].

III. ENERGY-BASED CONTROL FOR UPFCs

We apply the notion of incremental energy and dissipativity [6] to define a controller for the UPFC. The main task is to ensure convergence of states of interest to their desired (nominal) values. This problem is addressed via a Lyapunov-type design in terms of incremental quantities (denoted with tildes, e.g., $\tilde{x}$), selecting the control inputs that ensure the negative definiteness of the desired energy function.

For this purpose, let us consider the following energy function [6]

$$W = \underbrace{\frac{1}{2}L_p(\tilde{i}_{pd}^2+\tilde{i}_{pq}^2)}_{W_p} + \underbrace{\frac{1}{2}L_{\ell T}(\tilde{i}_{sd}^2+\tilde{i}_{sq}^2)+\frac{1}{2}C_\ell(\tilde{u}_{\ell d}^2+\tilde{u}_{\ell q}^2)}_{W_s} + \underbrace{\frac{1}{2}C(\tilde{u}_{c1}^2+\tilde{u}_{c2}^2)}_{W_{dc}} \qquad (9)$$

where tilde quantities are the (not necessarily small) increments respect to the nominal references (i.e. $\tilde{i}_{pq} = i_{pq} - i_{pq}^{ref}$).

As normally performed by conventional control strategies for STATCOMs and UPFCs [9], we assume that regulation of shunt ac currents is much faster than regulation of dc voltages. The active power reference current i_{pq}^{ref} of the shunt converter is, therefore, a control variable for the dc voltage regulation which ensures the power balance between the series and the shunt part of the UPFC. Thanks to this decoupling, we are allowed to impose separately the decrease of the three energy terms (W_p, W_s, W_{dc}) of (9) by proper control actions.

For example, using (1) and (9), it can be verified that:

$$\frac{d}{dt}W_p = -R_p\,\tilde{i}_{pd}^2 - \tilde{e}_{pd}\,\tilde{i}_{pd} - R_p\,\tilde{i}_{pq}^2 - \tilde{e}_{pq}\,\tilde{i}_{pq}. \qquad (10)$$

In order to make (10) negative, we can simply select the control input to be:

$$\tilde{e}_{pk} = K_{Idiss}\,\tilde{i}_{pk} \qquad k = d,q \qquad (11)$$

where K_{Idiss} is a positive design constant. The theoretical steady state values of the control inputs can be obtained from (1). However, it is not possible, in practice, to evaluate precise steady-state values due to model and parameters uncertainties. We can compensate for such errors introducing an estimation of *constant* parameters, possibly together with a feedforward action (e_{ffd}, e_{ffq}), by setting:

$$e_{pk} = \tilde{e}_{pk} + e_{ffk} + \Delta\hat{e}_{pk} \qquad k = d,q \qquad (12)$$

where $e_{ffd} = e'_{\ell d} - \omega_\ell L'_p\, i_{pq}$ and $e_{ffq} = \omega_\ell L'_p\, i_{pd}$, while $\Delta\hat{e}_{pd}$, $\Delta\hat{e}_{pq}$ are the estimators of the *constant* uncertainties ($\Delta e_{pd}, \Delta e_{pq}$) in the determination of the steady-state values, given by:

$$\frac{d}{dt}\Delta\hat{e}_{pk} = K_o^{-1}\,\tilde{i}_{pk} \qquad k = d,q \qquad (13)$$

where K_o is another positive design constant. Under these conditions, we are now able to guarantee the convergence of error terms to zero when the energy term W_p includes the parametric term:

$$W_{pT} = W_p + \frac{1}{2}K_o(\Delta e_{pd} - \Delta\hat{e}_{pd})^2 + \frac{1}{2}K_o(\Delta e_{pq} - \Delta\hat{e}_{pq})^2 \qquad (14)$$

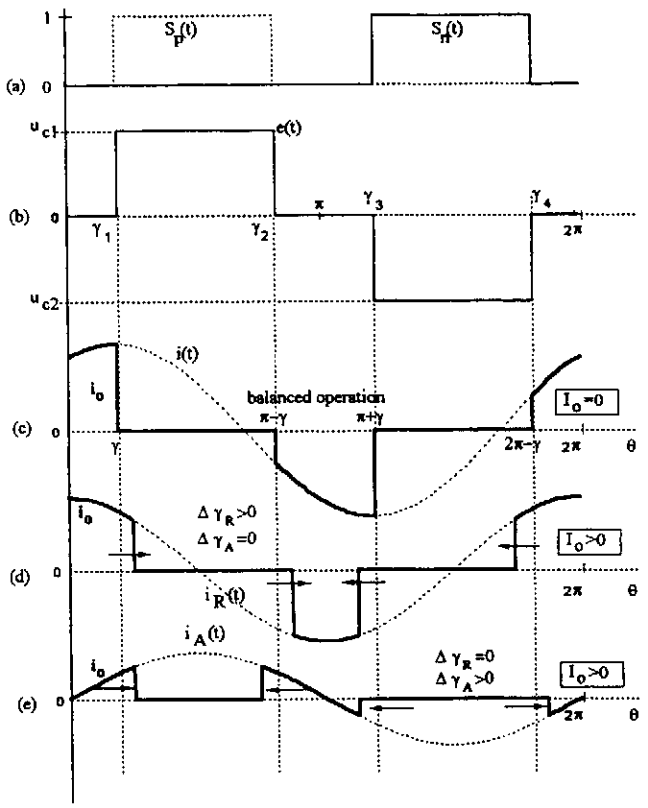

Fig. 3. NPC inverter: positive ($S_p(t)$) and negative ($S_n(t)$) switching functions; output voltage $e_a(t)$, phase current i(t), phase current active component $i_A(t)$, phase current reactive component $i_R(t)$, neutral current $i_o(t)$.

It is worth noting that:

- the control is globally stable even if the decoupling between the d-axis and q-axis introduced by the feedforward is not exact ($L_p' \neq L_p$)
- in this simple example, the control (10), (12-13) is linear and standard techniques can be used to determine design parameters K_{Idiss} and K_o.

A similar approach can be applied for the control of the series part of the UPFC or, equivalently, of the energy term W_s, leading to control equations very similar to (10-13). Instead, focusing on dc voltage regulation, we can show, using (3) and (9), that:

$$\frac{d}{dt}W_{dc} \leq \frac{\tilde{u}_{cT}}{u_{cT}}\left[e_{\ell d} i_{pd}^{ref} + \sum_{k=d,q} e_{sk} i_{sk}\right] - i_{oT}\frac{u_c^{ref}}{u_{cT}}\left(\tilde{u}_{c1} - \tilde{u}_{c2}\right) \quad (15)$$

In order to make (15) negative, we can select active current reference i_{pq}^{ref} and deviation angles $\Delta\gamma_A$ and $\Delta\gamma_R$ to be:

$$\begin{aligned} i_{pd}^{ref} &= -\frac{\sum_{k=d,q} e_{sk}\, i_{sk}}{e_{\ell d}} - K_{Udiss}\frac{u_{cT}}{e_{\ell d}}\tilde{u}_{cT} \\ \Delta\gamma_A &= +K_A I_{AT}\left(\tilde{u}_{c1} - \tilde{u}_{c2}\right) \\ \Delta\gamma_R &= -K_R I_{RT}\left(\tilde{u}_{c1} - \tilde{u}_{c2}\right) \end{aligned} \quad (16)$$

where K_{Udiss}, K_A and K_R are positive constants, and I_{AT} and I_{RT} the total active and reactive phase currents (see Fig. 3) evaluated from the reference currents. Note that an estimation procedure similar to (13-14) can be applied to cope with the (small) steady-state errors on the dc voltages, if needed.

It is worth noting that the energy-based approach, here presented, leads to a control law which is similar to the conventional approach reported in [9], as long as we restrict this consideration to ac currents control, due to the assumed decoupling between the dc voltages and ac currents control. However, without this assumption, which has been used here for simplicity, we are able to derive a new family of non-linear controllers for the non-linear dynamic equations (1-3) which results in globally stable behaviour, robustness against parameter variations and, more importantly, allows a reduction of the dc capacitor storage capability, since the speed of response of the voltage loop can be made comparable to that of the current loop. Investigation of these properties is still under progress and will be reported in the future.

IV. ATP MODELING

The main circuit of the UPFC, the transmission line and the generators are modeled with components in the branch data and in the switch data, while all the control processing and signal generation are modeled with TACS components.

The model, adopted in this paper, consist of a 24-pulse inverter, instead of the actual 48-pulse [8], to reduce model complexity. Each inverter module uses type-11 switches to represent GTO switches, reverse-connected diodes and clamp diodes. The magnetic coupling of the multi-pulse transformer replicates the typical zig-zag arrangement; however, the leakage impedance has been approximated by a single lumped impedance on the transmission line side of the multipulse transformer.

A good approximation of the described system can be obtained substituting each inverter leg with voltage sources on the ac side and current sources on the dc side, both properly driven by:

$$\begin{aligned} e(t) &= S_p(t)u_{c1}(t) - S_n(t)u_{c2}(t) \\ i_1(t) &= S_p(t)i(t) \\ i_2(t) &= -S_n(t)i(t) \end{aligned} \quad (17)$$

where $S_p(t)$ and $S_n(t)$ are the switching functions shown in Fig. 3a. Indeed, after several comparisons, we didn't find any significant difference between the circuit oriented approach of the NPC inverters and the approximations obtained with the switching functions, provided that the integration step was set smaller than 1μs. Moreover, the introduced approximation (17), besides allowing faster simulation time thanks to the reduced complexity and the possible higher integration step, allows the elimination of the multipulse transformer, since magnetic coupling can be included in the generation of the switching functions.

In order to cope with long simulation times, we have also considered the time-averaging of the switching variable of (17). In this case, NPC inverters are represented with controlled fundamental voltage sources on the ac side and controlled fundamental current sources on the dc side. The approximations involved in the time averaging, which allow integration step up to 30-50μs and a UPFC model more suitable for testing damping of low-frequency oscillations and transient stability improvement, are quantified in Section V.

V. SIMULATION RESULTS

The configuration we chose in order to verify UPFC performance is shown in Fig. 4 (system parameters are given in the Appendix). It represents a single machine connected to an infinite bus through two transmission lines; in line *(a)* a UPFC, rated at 20% of the nominal power of the generator, is inserted. For the initial test of the UPFC *internal* control, we have preliminarily imposed the voltages in bus A and bus B, reproducing two infinite bus at point A and B.

In these conditions, the performance of the UPFC in the presence of step changes of the reference currents

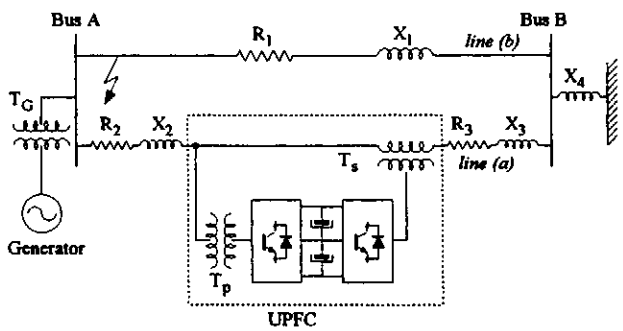

Fig. 4. Test case.

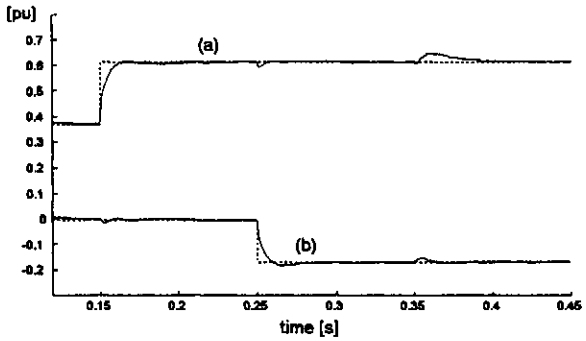

Fig.5. Serie currents: (a) d-axis (active) current and its reference (dotted line); (b) q-axis (reactive) current and its reference (dotted line);

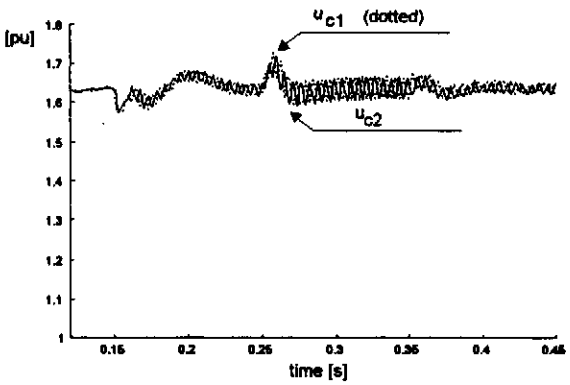

Fig.7. Dc link voltage capacitors.

(i_{pd}^{ref}, i_{sq}^{ref}, i_{sd}^{ref}) is shown in Figs. 5-9. At 0.15s there is a step reference variation of the series active currents from 0.37pu to 0.61pu (series currents and voltages and dc voltages are referred to P_N=160MVA and V_{b1}=37kV base, while shunt currents and voltages to P_N=160MVA and V_{b2}=138kV base). After 100ms, there is a step variation of the series reactive currents from 0 to -0.17pu and finally, at 0.35s the shunt reactive reference is changed from -0.04pu to 0.55pu. Fig. 5 and Fig. 6 show the series and shunt currents, together with their references, following the described transients, while Fig. 7 shows the dc voltage capacitors. Note that the UPFC is able to regulate the desired currents within a line cycle and the dc voltages within few cycles. Trace (c) of Fig. 6 shows also the instantaneous power injected by the series converter, which corresponds, as expected, to the active power current of the shunt converter (trace (a)). Finally, Fig. 8 shows the instantaneous voltages injected by the series inverter. Note that the d-axis voltage (real voltage) controls the series reactive (power) current and the q-axis voltage (reactive voltage) control the series active (power) current.

In order to test the control of the midpoint voltage, we introduced 50μs asymmetry on the firing pulse which leads to different capacitor voltages as shown in Fig. 10. The deviation angles $\Delta\gamma_A$ and $\Delta\gamma_B$ are null up to 0.2s and at that time we applied rules (16)-b and (16)-c, which allow voltage equalization within 50ms. It is worth noting before 0.2s the shunt currents i_{pd} and i_{pq}, even if controlled at the correct dc value, show a non-negligible 3rd harmonic distortion, which disappear when capacitor voltages are equal. In fact, when the dc capacitor voltages are not equal, the output voltages of each converter have some harmonic components (even 2nd harmonics) which cannot be eliminated by the multipulse transformer. The dominant 2nd harmonic in the a-b-c reference frame causes the 3rd harmonic in the d-q reference frame shown in Fig. 9.

In order to quantify the difference between detailed simulations and time-averaged simulations, we show Fig. 10 where the results of both models are reported in presence of step variation of the shunt reactive current reference (from 0.5pu to -0.5pu) at 0.1s. As expected, the difference is quite small and negligible for power system studies.

With the time-averaged model of the UPFC we test the configuration of Fig.4. To initiate a power oscillation in this simple test case, a fault is assumed at bus A occurring from 2s to 2.2s. Different configurations have been tested starting from the same initial condition where the generator output power is 4pu, line (a) carries 1.6pu active power and line (b) 2.4pu. Initially the UPFC is kept off and the generator phase angle, following the disturbance, is shown in the trace (a) of Fig.11. Instead, trace (b) reports the effect of turning on the UPFC driven with a *constant* series power reference of 1.6pu. As expected, the oscillation is less damped since the UPFC holds the power flow on its line constant, subtracting, respect to the

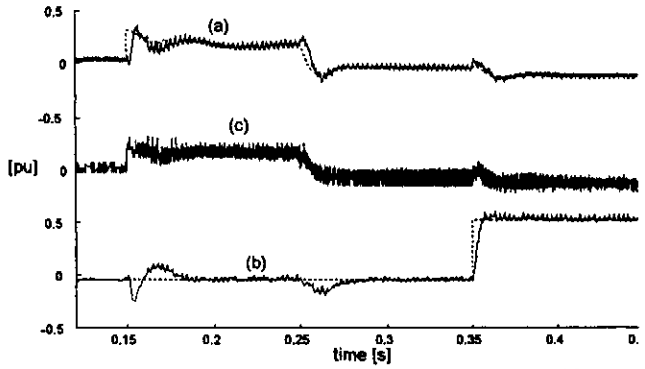

Fig. 6. Shunt currents: (a) d-axis (active) current and its reference (dotted line); (b) q-axis (reactive) current and its reference (dotted line); (c) instantaneous active power injected by the series inverter.

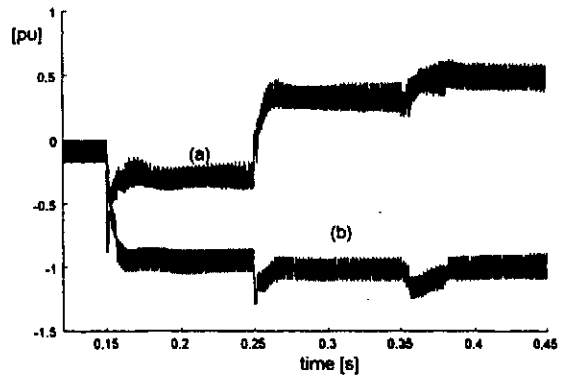

Fig. 8. Instantaneous voltage injected by the series converter: (a) d-axis voltage; (b) q-axis voltage;

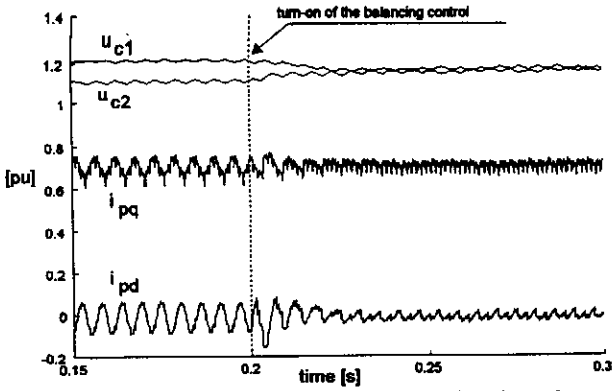

Fig. 9. Performance of the control of the midpoint voltage.

previous case, some oscillating power needed to synchronise the generator. Finally, we set a variation of the active power reference to be proportional to the derivative transmission line angle, here derived from the estimated voltage drop between bus A and bus B, obtained from the *local* variables e_{sd}, e_{sq}, i_{sd} and i_{sq}. In these conditions, we obtain the waveform (c) of Fig. 11, which shows the capability of the UPFC to damp system oscillations. Indeed, this is just an example of possible control law for the UPFC and many other solutions [14,12,13] can be investigated for optimizing the UPFC interaction with the power systems.

VI. CONCLUSIONS

The paper has described the mathematical analysis and proposed a control structure for a UPFC based on multipulse NPC Inverters. Attention has been focused on an energy-based approach to the control design for both shunt and series converter, together with a new solution for the regulator of the dc link voltage sharing across dc capacitors of the multilevel inverters. This approach has been tested using a detailed UPFC simulation model, developed in ATP using 24-pulse NPC inverters and, subsequently, approximated by switching and time-averaged functions. Simulation results have verified UPFC dynamic performance, effects of increasing transmission capacity and damping of low-frequency oscillations.

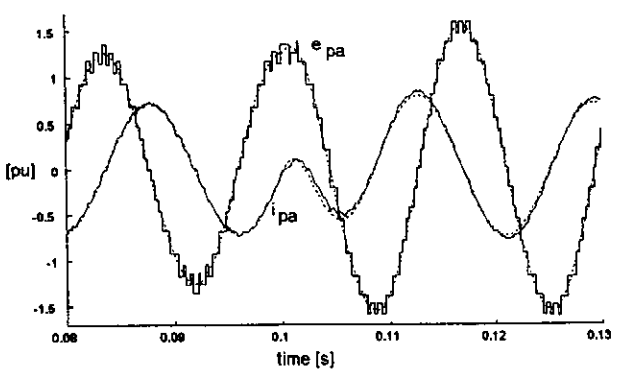

Fig. 10. Details of a step variation of reactive power absorbed by the shunt converter: comparison between detailed simulation (solid line) and time-averaged simulation (dotted line).

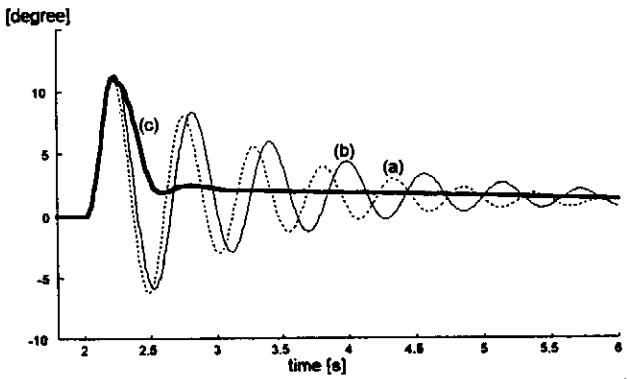

Fig. 11. Generator phase angle following a fault in bus A which starts at 2s and ends at 2.2s: (a) (dotted) without UPFC, (b) using the UPFC working at constant active power reference, (c) (thick line) using the UPFC with damping function.

VII. APPENDIX

Nominal power of UPFC = 160MVA
Nominal power of the generator = 800MVA (speed governors are neglected)
Transformer T_G: S_N=800MVA, $v_{cc\%}$=12%, H=3.1 s
Transformer T_P: S_N=160MVA, V_{1N}/V_{2N}=138kV/37kV, $v_{cc\%}$=15%
Transformer T_S: S_N=160MVA, V_{1N}/V_{2N}=37kV/37kV, $v_{cc\%}$=15%
Transmission line voltage: V_t=138kV
X_4=0.05pu R_2=0.012pu; X_2=0.28pu; R_1=R_3=0.037pu; X_1=X_3=0.56pu; C=0.26pu (Based quantities: P_b=160MVA, V_b=37kV)

VIII. REFERENCES

[1] IEEE. Facts Applications. *IEEE press 96-TP-116*, 1996.

[2] L. Gyugyi, "A Unified Power Flow Control Concept for Flexible AC Transmission Systems" ", *IEE Proc.-C*, Vol. 139, No. 4, July 1992.

[3] L. Gyugyi, et at. "The Unified Power Flow Controller: A new Approach to Power Transmission Control", *IEEE Trans. on Power Delivery*, Vol. 10, No. 2, April 1995, pp. 1085-1097.

[4] K.K.Sen, E.J. Stacey, "UPFC-Unified Power Flow Controller: Theory, Modeling, and Applications ", *IEEE Trans. on Power Delivery*, Vol. 13, No. 4, October 1998, pp. 1453-1460.

[5] A. N.-Niaki, M.R. Iravani "Steady-State and dynamic models of Unified Power Flow Controller (UPFC) for Power System Studies" *96 WM 257-6-PWRS.*

[6] S.R. Sanders and G.C. Verghese, "Lyapunov-based Control for Switched Power Converters ", *IEEE Trans. on Power Electronics*, Vol. 7, No. 1, January 1992, pp. 17-24.

[7] Y. Chen, B. Mwinyiwiwa, Z. Wolanski, B.T. Ooi, "Regulating and Equalizing DC Capacitance voltages in Multilevel Statcom", *IEEE Trans. on Power Delivery*, Vol. 12, No. 2, April 1997, pp. 901-907.

[8] C. Shauder, et. al "AEP UPFC Project: Installation, Commissioning and Operation of the ±160MVA Statcom (Phase I)", *IEEE Trans. on Power Delivery*, Vol. 13, No. 4, October 1998, pp. 1530-1535.

[9] C. Shauder, H. Mehta, "Vector Analysis and Control of Advanced Static Var Compensators ", *IEE Proc.-C*, Vol. 26, No. 4, July 1993, pp. 299-306.

[10] C. Shauder, et. al "Operation of the Unified Power Flow Controller (UPFC) under Practical Contraints", *IEEE Trans. on Power Delivery*, Vol. 13, No. 2, April 1998, pp. 630-639.

[11] E. Joncquel, X. Lombard, "A Unified Power Flow Controller Model for the Electromagnetic Transients Program " *European Power Electronics (EPE) Conf*, Sevilla 1995, pp. 2.173-2.178.

[12] R. Caldon, A. Mari, A. Paolucci, R. Turri, "Power Requirements Assessment of FACTS Devices by Static and Dynamic Modelling " EPSOM'98, Zurich, September 1998, pp. 9.1-9.6.

[13] M. Noroozian, et al. "Series-connected FACTS devices control strategy for damping electromechanical oscillations " 12th PSCC, Dresden, August 1996.

[14] K.R. Padiyar, A.M. Kulkarni, "Control Design and Simulation of Unified Power Flow Controller", *IEEE Trans. on Power Delivery*, Vol. 13, No. 4, October 1998, pp. 1348-1354.